

The Outer Halo Globular Clusters of M31^{*}

Alan Alves-Brito^{1†}, Duncan A. Forbes¹, Jon T. Mendel¹, George K.T. Hau¹
and Michael T. Murphy¹

¹*Centre for Astrophysics and Supercomputing, Swinburne University of Technology, Hawthorn, Victoria 3122, Australia*

Accepted 1988 December 15. Received 1988 December 14; in original form 1988 October 11

ABSTRACT

We present Keck/HIRES spectra of 3 globular clusters in the outer halo of M31, at projected distances beyond ≈ 80 kpc from M31. The measured recession velocities for all 3 globular clusters confirm their association with the globular cluster system of M31. We find evidence for a declining velocity dispersion with radius for the globular cluster system. Their measured internal velocity dispersions, derived virial masses and mass-to-light ratios are consistent with those for the bulk of the M31 globular cluster system. We derive old ages and metallicities which indicate that all 3 belong to the metal-poor halo globular cluster subpopulation. We find indications that the radial gradient of the mean metallicity of the globular cluster system interior to 50 kpc flattens in the outer regions, however it is still more metal-poor than the corresponding field stars at the same (projected) radius.

Key words: globular clusters: general, galaxies: individual: M31, galaxies: star clusters.

1 INTRODUCTION

One of the great unanswered questions in astrophysics is the formation and evolution of galaxies in the Universe. Since M31 is our closest spiral galaxy, located at a distance of ~ 780 kpc (Holland 1998), it is considered an ideal astrophysical laboratory to test the different ideas about galaxy formation and evolution.

In particular, the outer regions of galaxies are expected to hold a wealth of information about the way in which galaxies are assembled. For example, in order to explain how the Milky Way was formed, Eggen, Lynden-Bell & Sandage (1962) and Searle & Zinn (1978) studied the kinematics and metallicity of stars and globular clusters in the bulge/halo of the Milky Way. While the former suggested the Galactic halo formed during a rapid ($\sim 10^8$ years) monolithic collapse of a gaseous protocloud, the latter suggested formation via the accretion and merging of independent protogalactic fragments over a longer dynamical timescale (10^9 years). Importantly, Searle & Zinn’s (1978) seminal paper on Galactic globular clusters constitutes the basis for modern ideas re-

lating to the formation of cosmological large scale structures in the universe (e.g. White & Rees 1978).

Perhaps the main difference between the globular cluster systems of M31 and the Milky Way is that the former is more populous with an estimated total of ~ 450 members (Barmby et al. 2000; Perrett et al. 2002; Huxor et al. 2008; Caldwell et al. 2009) and may contain a significant population of intermediate age (3–6 Gyr) globular clusters. Otherwise they share many similarities: a Gaussian-like luminosity function that peaks around $M_V = -7.62$ mag with a dispersion of 1.06 mag (Barmby, Huchra & Brodie 2001); two subpopulations of mean metallicity $[\text{Fe}/\text{H}] = -1.57$ and -0.61 associated with the halo and bulge, respectively (Barmby, Huchra & Brodie 2001; Forbes, Brodie & Larsen 2001); and similar structural properties (Barmby et al. 2007).

A relevant recent discovery is that of a metal-poor stellar halo in M31 (Kalirai et al. 2006; Chapman et al. 2006). At projected radii beyond 60 kpc Kalirai et al. (2006) estimate a mean halo metallicity of $[\text{Fe}/\text{H}] = -1.26$, which decreases to -1.48 if an $[\alpha/\text{Fe}]$ abundance ratio similar to the Milky Way’s stellar halo is assumed. Beyond a projected radius of 70 kpc, outer halo globular clusters in M31 have also been discovered recently but remain rare, these include 1 globular cluster reported in Martin et al. (2006), 2 in Mackey et al. (2007), 2 in Galleti et al. (2007) and 1 in Huxor et al. (2008).

In this Letter, we present Keck spectra for some of the

^{*} Based on observations obtained at the W. M. Keck Observatory, which is operated as a scientific partnership among the California Institute of Technology, the University of California, and the National Aeronautics and Space Administration.

[†] E-mail: abrito@astro.swin.edu.au (AAB)

Table 1. Properties for the 3 outer globular clusters.

Properties*	GCM06	GC5	GC10
(1)	(2)	(3)	(4)
R.A. [J2000]	00:50:42.5	00:35:59.7	01:07:26.4
Dec. [J2000]	32:54:59.6	35:41:03.6	35:46:49.7
E_{B-V} [mag]	0.08	0.08	0.09
r_h [pc]	2.3 ± 0.20	6.3 ± 0.15	4.3 ± 0.15
$M_{V,o}$ [mag]	-8.5 ± 0.3	-8.8	-8.3
R_p [kpc]	100	78.5	99.9

Notes.— (*) As given in Martin et al. (2006) and Mackey et al. (2007).

furthest projected distant (R_p) globular clusters known at this time in the halo of M31 — GC5 and GC10 (Mackey et al. 2007) and GCM06 (Martin et al. 2006). Two of them (GC5 and GC10) do not have spectroscopic information published to date. Thus, we present, for the first time, their kinematics, structural parameters, ages and spectroscopic metallicities. We briefly discuss our results within the context of the halo assembly of M31.

2 OBSERVATIONS AND DATA REDUCTION

The three globular clusters were selected from the imaging survey reported by Martin et al. (2006, GCM06) and Mackey et al. (2007, GC5 and GC10). The spectra were observed with the Keck/HIRES instrument (Vogt et al. 1994) on 2008 August 19. The instrument setup employed a $0''.86$ -wide, $7''.0$ -long slit, providing a spectral resolving power of $R \approx 50000$. The cross-disperser angle was set to cover wavelengths $\lambda\lambda = 4020\text{--}8520 \text{ \AA}$. For each globular cluster, 3×900 -s exposures were taken in succession, without any intervening re-acquisition sequences, with the slit oriented at the parallactic angle. Exposures were offset from each other in the direction perpendicular to the parallactic angle (i.e. along the horizon). The first exposure was centred on the globular cluster with the others offset either side of centre. The offsets were $1''.0$ for GC5 and GCM06 and $0''.8$ for GC10. The seeing was stable throughout the observations at $\sim 0''.8$.

Science and calibration data were reduced using the MAKEE (MAuna Kea Echelle Extraction) Keck Observatory HIRES Data Reduction Program, written by Tom Barlow. Bias frames, flat-fields, order trace and ThAr arc images were taken as part of the Keck base calibrations. The final reduction process comprised bias-subtraction and flat-fielding, using base calibrations which were previously co-added. The wavelength calibration was carried out with solutions obtained from the ThAr arc exposures, which provided typical mean residuals of 0.05 \AA . Spectra were then cosmic ray cleaned, sky-subtracted and extracted into a series of heliocentric corrected 2D spectra with no correction to a vacuum wavelength scale applied. The spectra were then combined with inverse variance weighting to yield the final spectrum of each cluster. Basic properties for the 3 globular clusters are given in Table 1. Figure 1 displays a portion of the final spectra indicating the data quality.

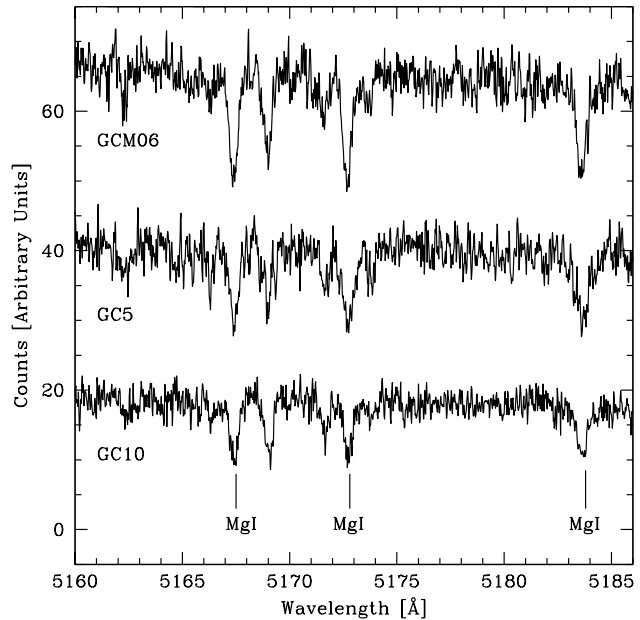


Figure 1. Integrated-light Keck/HIRES spectra of the 3 globular clusters around the Mg b Triplet wavelength region. The prominent absorption MgI lines are labeled just below the spectra. The typical signal-to-noise per pixel is 20 at this wavelength region.

3 DATA ANALYSIS

The galactocentric coordinates (X, Y) and projected distances for our 3 outer halo globular clusters were calculated relative to an adopted M31 central position of $\alpha_{J2000} = 00^{\text{h}}42^{\text{m}}44^{\text{s}}.31$, $\delta_{J2000} = +41^{\circ}16'09''.4$. The position angle for the X-coordinate is 38° (Kent 1989), and we adopt 780 kpc as the distance to M31 (Holland 1998). At this distance, $1'$ corresponds to 228 pc. The projected distances calculated in this way are similar to those quoted in Table 1 from colour magnitude diagram (CMD) studies. These calculated radii are used throughout this paper to facilitate comparison with other literature work.

The velocity dispersions (σ) and heliocentric radial velocities (v_{\odot}) were obtained by fitting the observed spectra with the convolution of suitable template spectra of giant stars taken with the same telescope and instrument and with a Gaussian velocity profile using the program `pixfitgau` (see van der Marel & Franx 1993 for more details). The best fitting parameters are obtained by χ^2 -minimisation procedures. We used the spectral region $5150\text{--}5240 \text{ \AA}$, where strong features permit a reliable determination of the velocity dispersion. The velocity dispersions were also measured using the spectral region $5370\text{--}5420 \text{ \AA}$, which contains many iron lines. The results were consistent displaying differences of less than 1 km s^{-1} . The adopted values are based on the $5150\text{--}5240 \text{ \AA}$ spectral region. The uncertainties quoted are only due to the random noise, that is, by taking into account the CCD read-out noise per pixel ($\sim 0.6 \text{ e}^-/\text{pix}$) and gain (1.9 e^-).

The globular cluster masses were computed by using the Virial Theorem, being $M = 10 \times \sigma^2 r_h / G$, where σ is the velocity dispersion, r_h is the half-light radius, G is the grav-

itational constant and a virial coefficient of 10 was used (see Forbes et al. 2008). For GC5 and GC10 the r_h values were measured using images obtained with the Advanced Camera for Surveys on Hubble Space Telescope (Mackey et al. 2007), while for GCM06 it was obtained using ground-based observations (Martin et al. 2006).

Spectroscopic metallicities were obtained by using metallicity calibrations from Mgb and CH (Brodie & Huchra 1990; Perrett et al. 2002) and for $Mg2$ (Brodie & Huchra 1990; Buzzoni, Gariboldi & Mantegazza 2002) indices. In addition, we also employed the robust approach of Proctor, Forbes & Beasley (2004), which performs the simultaneous χ^2 -minimisation of a large number of spectral indices. This method leverages the entire suite of available indices to estimate stellar population parameters and, in particular, makes apparent those indices which deviate from the general trend of the data, effectively eliminating errors in calibration or the spectra themselves (e.g. sky-line contamination, bad pixels etc).

The Single Stellar Population (SSP) models used here are from Thomas, Maraston & Korn (2004), which have been used to recover reliable ages and metallicities for both Galactic and extragalactic globular clusters (e.g. Mendel, Proctor & Forbes 2007; Beasley et al. 2008). However, we note that such an analysis is usually applied to much lower resolution data than obtained here. Hence, absorption line indices were measured after broadening the spectra to the wavelength dependent Lick/IDS system resolution as described in Worthey & Ottaviani (1997). The Lick index definitions were taken from Worthey & Ottaviani (1997) and Trager et al. (1998).

4 RESULTS AND DISCUSSION

We derive a heliocentric radial velocity of -358.3 ± 1.9 km s^{-1} for GC5, $v_{\odot} = -291.2 \pm 2.1$ km s^{-1} for GC10 and a value of -354.7 ± 2.2 km s^{-1} for GCM06. All 3 globular clusters are consistent with being part of the M31 ($v_{\odot} = -300$ km s^{-1}) globular cluster system. Recently, using a low-resolution spectrum ($R \sim 1300$), Galleti et al. (2007) determined $v_{\odot} = -312 \pm 17$ km s^{-1} for GCM06. This mean difference between the heliocentric radial velocities suggests the errors quoted in the lower resolution work may have been underestimated.

As shown in Fig. 2 our radial velocity results are clustered around M31's systemic recession velocity of -300 km s^{-1} . Regarding this issue, Chapman et al. (2006) analysed a large sample of red giant branch stars in the halo of M31 (between $10 \leq R_p \leq 70$ kpc) and fitting a simple model to the observed data they obtained the dispersion of the radial velocity as a function of the projected radius R_p ¹. Their linear relation implies $\sigma_{v_{\odot}} = 62$ km s^{-1} at 100 kpc distance from the centre of M31. Combining the velocity results for the 5 globular clusters beyond $R_p = 70$ kpc presented in Fig. 2, we derive a velocity dispersion of 65 km s^{-1} in the outer halo of M31. For the Milky Way globular cluster system, Battaglia et al. (2005) found that the radial velocity dispersion shows a nearly constant value of 120 km s^{-1} out

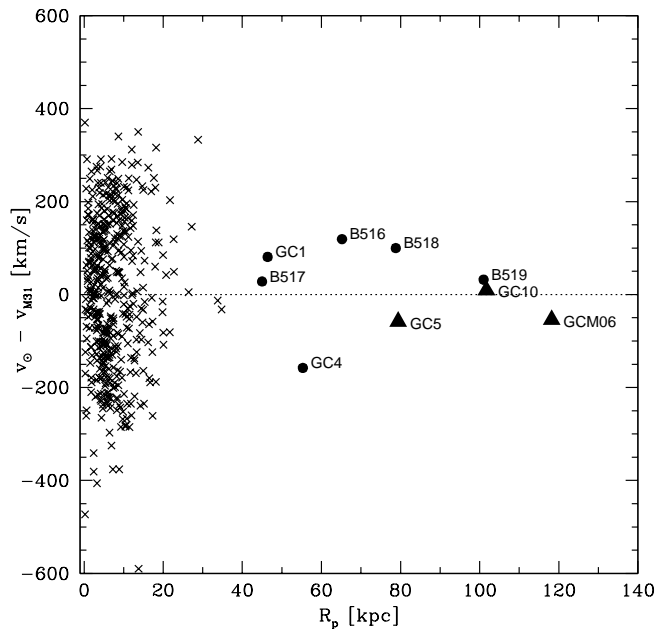


Figure 2. Heliocentric radial velocities for M31 globular clusters corrected to the M31 velocity frame against the projected radius. Symbols are as follows: the crosses for globular clusters at $R_p \leq 40$ kpc, while the solid symbols are for those at large projected distances ($R_p \geq 40$ kpc). The present sample is represented by solid triangles, while the outer globular clusters of Galleti et al. (2007) and Mackey et al. (2007) are represented by the solid circles.

to 30 kpc, which declines down to 50 km s^{-1} at about 120 kpc. The declining velocity dispersion in the outer halo suggests a relatively low mass halo, in which the virial velocity of the halo is less than the rotation speed of the disk (Abadi, Navarro & Steinmetz 2006), similar to that proposed for the Milky Way by Klypin, Zhao & Somerville (2002).

In Fig. 3 we show the measured globular cluster internal velocity dispersion versus the absolute visual magnitude. It is evident that our 3 outer globular clusters resemble those found for Galactic globular clusters (Pryor & Maylan 1993) and also for other globular clusters in M31 (Barmby et al. 2007). Such a scaling relation is not well understood to date. Yet, as briefly discussed by Djorgovski (1991, 1993), the primordial L - σ relation (slope ~ 1) of young globular clusters would be affected by subsequent dynamical processes (tidal shocks, for example), which would lead to the L - σ power-law relation observed by the present day.

For our sample, the dynamical mass-to-light ratio in the V band M/L_V ranges from 1.50 to 4.51 (in solar units). Our results are in agreement with those obtained by Dubath & Grillmair (1997) for nine M31 globular clusters ($1.0 \leq M/L_V \leq 6.5$). In addition, Pryor & Meylan (1993) obtained a mean dynamical $M/L_V = 2.3 \pm 1.1$ for the Galactic globular cluster system. Hence, within the uncertainties, GCM06 and GC5 display typical Galactic globular cluster M/L_V ratios, while GC10 is rather on the high side.

When compared to the Galactic globular cluster system, one remarkable aspect of the M31 globular cluster system is its large range in age. That is, while the Milky Way presents a very homogeneous old population, M31 displays a

¹ $\sigma_{v_{\odot}}(R_p) = 152 - 0.90R_p$ km s^{-1} , with R_p given in kpc.

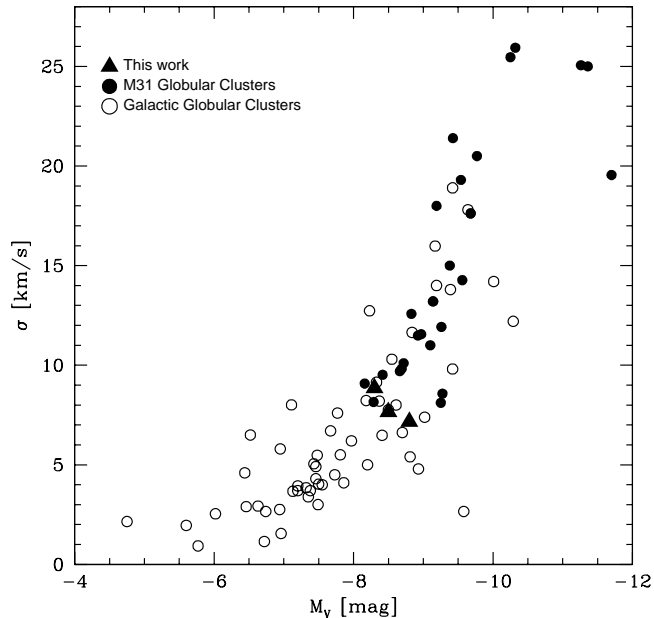


Figure 3. Internal velocity dispersion as a function of the absolute visual magnitude for the present sample (*triangles*), Galactic globular clusters (*open circles*) and for other globular clusters in M31 (*solid circles*). Refer to the text for references.

Table 2. Derived parameters for the 3 outer globular clusters.

ID	R_p [kpc]	σ [kms $^{-1}$]	M [$10^5 M_\odot$]	M/ L_V [M_\odot/L_\odot]	Age [Gyr]
(1)	(2)	(3)	(4)	(5)	(6)
GCM06	118.2	7.7 ± 0.4	3.14 ± 1.57	1.50 ± 0.75	7.1 ± 3.0
GC5	79.4	7.2 ± 0.4	7.51 ± 1.50	2.73 ± 0.54	10.0 ± 3.0
GC10	101.7	8.8 ± 0.7	7.83 ± 1.56	4.51 ± 0.90	12.6 ± 3.0

young population (≤ 2 Gyr), a number of intermediate age globular clusters (3-6 Gyr) and old globular clusters (≥ 7 Gyr) as well (e.g. Beasley et al. 2005). Based on our stellar population analysis, we found that the present outer halo globular clusters of M31 have a mean age of around 10 ± 3 Gyr. This mean spectroscopic age determination is in agreement with the color-magnitude diagrams presented in Martin et al. (2006) and Mackey et al. (2007) for these globular clusters. Furthermore, our dynamical mass-to-light ratios ($M/L_V \geq 1.5$) are compatible with an old stellar population. Our final derived parameters are summarized in Table 2.

Spectroscopic metallicities for outer metal-poor globular clusters are essential to the scenarios of chemical enrichment of the halo in galaxies since these objects are considered halo-tracers. In Table 3 we present our spectroscopic metallicity determinations and, for comparison, the photometric metallicities. The final metallicities were computed as the median of the different spectroscopic values presented in Table 3, with a robust uncertainty of $1.5 \times \text{SIQR}$ (Semi-InterQuartile Range) being adopted. This lead to $[\text{Fe}/\text{H}] = -1.37 \pm 0.15$ dex for GCM06, $[\text{Fe}/\text{H}] = -1.33 \pm 0.12$ dex for

Table 3. Metallicity determinations for the 3 outer globular clusters.

Method	GCM06	GC5	GC10
χ^2	-1.65 ± 0.10	-1.40 ± 0.10	-1.73 ± 0.10
Mgb *,a	-1.56 ± 0.11	-1.74 ± 0.08	-1.82 ± 0.08
CH *,b	-1.37 ± 0.25	-1.24 ± 0.25	-1.81 ± 0.24
Mg2 *,c	-1.36 ± 0.05	-1.33 ± 0.06	-1.54 ± 0.01
CMD d	-1.30 ± 0.15	-1.84 ± 0.15	-2.14 ± 0.15
Adopted	-1.37 ± 0.15	-1.33 ± 0.12	-1.73 ± 0.20

Notes.— (*): Average values using different calibrations as follows : (a),(b): Brodie & Huchra (1990) and Perrett et al. (2002); (c): Brodie & Huchra (1990) and Buzzoni et al. (1992); (d): Isochrone fitting from Martin et al. (2006) and Mackey et al. (2007).

GC5 and $[\text{Fe}/\text{H}] = -1.73 \pm 0.20$ dex for GC10. These values, taking all uncertainties into account, are consistent with the CMD ones reported in Table 3 for GC10 and GCM06, while GC5 is a factor of 3 more metal-rich than the CMD estimate. Note, however, that although the metallicity quoted for GC5 based upon the *Mgb* method is also supported by visual inspection of the high-quality spectra shown in Fig. 1, the higher value obtained by the median of the different spectroscopic measurements was adopted.

Both the photometric and spectroscopic methods have their advantages and disadvantages. Whilst the former is reddening and distance-modulus dependent, the latter is calibration and model-dependent. Furthermore, photometric metallicities are also susceptible to the set of isochrones used as well as to age-metallicity degeneracy on the red giant branch. On the other hand, measurements of age, metallicity and elemental abundance from integrated spectra using a single index or pairs of orthogonal indices (e.g. $H\beta$ vs. $[\text{MgFe}]$) are especially susceptible to index calibration errors, a particular concern for our uncalibrated data.

In Fig. 4 we present the behaviour of the mean metallicity as a function of the projected radii in the halo of M31 using our metal-poor globular cluster sample, together with additional values from the literature for field stars and globular clusters. Three main aspects are illustrated in this figure. Firstly, there seems to exist a metallicity gradient for the metal-poor globular clusters at a projected distance less than 50 kpc from the centre of M31. Secondly, we find tentative evidence for the mean globular cluster metallicity to flatten off at $[\text{Fe}/\text{H}] \sim -1.6$, which is similar to the lower threshold seen in many other galaxies (e.g. Forbes et al. 2000). Thirdly, our results confirm that the globular clusters in M31 are systematically more metal-poor than their outermost counterpart field stars, bearing in mind that we may be sampling different physical radii. This point can be explained in the context of chemical pre-enrichment having taken place in M31 before most of the halo formation has occurred (Durrell, Harris & Pritchett 1994, 2001). Similar results have also been found for giant elliptical galaxies (e.g. Harris, Harris & Poole 1999). However, Schorck et al. (2008) show that the metallicity distribution function of the Galactic halo field stars is indistinguishable from that of the Galactic globular cluster system.

Currently, it is not clear what fraction of the Milky Way's halo has been assembled via dissipational collapse (monolithic collapse and gas rich mergers), and which by dissipationless accretion. However, the global properties of the present-day globular clusters of the Milky Way suggest a scenario where the inner halo (within 10 kpc) was formed via dissipative collapse, while the outer halo has an accretion origin (e.g. Bica et al. 2006). The metallicity trend in Fig. 4 is also consistent with this picture. It suggests that the steep metallicity gradient for the globular cluster system of M31 in the inner halo flattens in the outer regions. Such a flattening could be indicative of the outer halo globular clusters being likely accreted from satellites during an early period of merging (see e.g. Font et al. 2006).

5 SUMMARY

In summary, we confirm that the 3 outer globular clusters in the present sample are kinematically members of the M31 globular cluster system and have structural parameters that, within the uncertainties, resemble those of the Milky Way globular clusters. Furthermore, they are characterized by an old stellar population (> 7 Gyr), whose mean metallicity matches the M31 metallicity peak for halo globular clusters (e.g. Barmby, Huchra & Brodie 2001). Unlike the Milky Way, we confirm that the outer halo globular clusters of M31 are systematically more metal-poor than their counterpart field stars (Kalirai et al. 2006) at a given projected radius. We also find evidence for a declining velocity dispersion with radius for the globular cluster system.

We note that the most distant globular cluster in the Milky Way, AM 1, lies at 120 kpc. It is reasonable to expect that more globular clusters in the outer halo of M31 will be discovered with time, which should be followed-up with integrated-light spectra.

ACKNOWLEDGMENTS

We would like to thank Adrian Malec for his support with the MAuna Kea Echelle Extraction Program on MAC Systems and Söeren Larsen for sending us template star observations and useful comments. We are grateful to Jay Strader and the anonymous referee for constructive comments and suggestions. AAB acknowledges CNPq for financial support 200227/2008-4 (PDE). DF and GKTH thank ARC for financial support.

REFERENCES

Abadi M., Navarro J., Steinmetz M., 2006, MNRAS, 365, 747
 Barmby P., Huchra J.P., Brodie J.P., Forbes D.A., Schroder L.L., Grillmair C.J., 2000, AJ, 119, 727
 Barmby P., Huchra J.P., Brodie J.P. 2001, AJ, 121, 1482
 Barmby P. et al., 2007, AJ, 133, 2764
 Battaglia G. et al, 2005, MNRAS, 364, 433
 Beasley M.A., Brodie J.P., Strader J., Forbes D.A., Proctor R.N., Barmby P., Huchra J.P., 2005, AJ, 129, 1412
 Beasley M. A., Bridges T., Peng E., Harris W.E., Harris G.L., Forbes D.A., Mackie G., 2008, MNRAS, 386, 1443

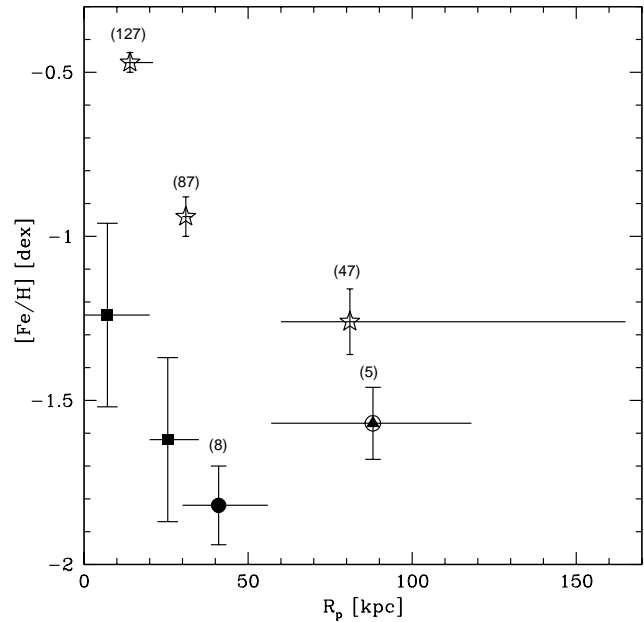


Figure 4. Mean metallicity plotted against the projected radius. Four different symbols are used: (i) red giant branch stars (*open stars*) from Kalirai et al. (2006); (ii) metal-poor globular clusters (*solid squares*) as analysed in Lee et al. (2008); (iii) metal-poor globular clusters (*solid circle*) from Mackey et al. (2006; 2007) and Galetti et al. (2007); (iv) metal-poor globular clusters (*solid circled triangle*) from this work and combined with those presented in Mackey et al. (2006) and Galletti et al. (2007) for EC4 ($[Fe/H] = -1.84$) and B518 ($[Fe/H] = -1.6$), respectively. Error bars correspond to the standard error on the mean $[Fe/H]$ measurements. When available, the total number of objects used is also indicated. The horizontal lines delineate the bin-size adopted.

Bica E., Bonatto C., Barbuy B., Ortolani S., 2006, A&A, 450, 105
 Brodie J. P., Huchra J. P., 1990, ApJ, 362, 503
 Buzzoni A., Gariboldi G., Mantegazza L., 1992, AJ, 103, 1814
 Caldwell N., Harding P., Morrison H., Rose J.A., Schiavon R., Kriessler J., 2009, AJ, 137, 94
 Chapman S. C., Ibata R., Lewis G.F., Ferguson A.M.N., Irwin, M., McConnachie A., Tanvir N., 2006, ApJ, 653, 255
 Djorgovski S., 1991, ASPC, 13, 112
 Djorgovski S., 1993, ASPC, 48, 496
 Dubath P., Grillmair C.J., 1997, A&A, 321, 379
 Durrell P.R., Harris W.E., Pritchett C.J. 1994, AJ, 108, 2114
 Durrell P.R., Harris W.E., Pritchett C.J., 2001, AJ, 121, 2557
 Eggen O. J., Lynden-Bell D., Sandage A. R., 1962, ApJ, 136, 748
 Font A. S., Johnston K.V., Bullock J. S., Robertson B.E. 2006, ApJ, 646, 886
 Forbes D.A., Masters K. L., Minniti D., Barmby P., 2000, A&A, 358, 471
 Forbes D.A., Brodie J.P., Larsen S.S., 2001, ApJ, 556, 83
 Forbes D.A., Lasky P., Graham A.W., Spitler L., 2008, MNRAS, 389, 1924

- Galletti S., Bellazzini M., Federici L., Fusi Pecci F., 2007, *A&A*, 471, 127
- Harris G.L.H., Harris W.E., Poole G.B., 1999, *AJ*, 117, 855
- Holland S., 1998, *AJ*, 115, 1916
- Huxor A.P., Tanvir N.R., Ferguson A.M.N., Irwin M.J., Iбата R., Bridges T., Lewis G.F., 2008, *MNRAS*, 385, 1989
- Kalirai J.S. et al., 2006, *ApJ*, 648, 389
- Kent S. 1989, *AJ*, 97, 1614
- Klypin A., Zhao H., Somerville R., 2002, *ApJ*, 573, 597
- Lee M.G., Hwang H.S., Kim S.C., Park H.S., Geisler D., Sarajedini A., Harris W.W., 2008, *ApJ*, 674, 886
- Mackey A.D. et al., 2006, *ApJ*, 653, 105
- Mackey A.D. et al., 2007, *ApJ*, 655, 85
- Martin N.F., Iбата R.A., Irwin M.J., Chapman S., Lewis G.F., Ferguson A.M.N., Tanvir N., McConnachie A.W., 2006, *MNRAS*, 371, 1983
- Mendel J.T., Proctor R.N., Forbes D.A., 2007, *MNRAS*, 379, 1618
- Proctor R.N., Forbes D.A., Beasley M.A., 2004, *MNRAS*, 355, 1327
- Perrett K.M., Bridges T.J., Hanes D.A., Irwin M.J., Brodie J.P., Carter D., Huchra J.P., Watson F.G., 2002, *AJ*, 123, 2490
- Pryor C., Meylan G., 1993, *ASPC*, 50, 357
- Searle L., Zinn R., 1978, *ApJ*, 225, 357
- Schoerck T. et al., 2008, preprint (astro-ph/0809.1172)
- Thomas D., Maraston C., Korn A., 2004, *MNRAS*, 351, 19
- Trager S. C., Worthey G., Faber S. M., Burstein D., Gonzalez J.J., 1998, *ApJS*, 116, 1
- van der Marel R.P., Franx M., 1993, *ApJ*, 407, 525
- Vogt S.S. et al., 1994, *SPIE*, 2198, 362
- White S.D.M., Rees M.J., 1978, *MNRAS*, 183, 341
- Worthey G., Ottaviani D.L., 1997, *ApJS*, 111, 377